NOTES AND CORRESPONDENCE

Warm Upper-Level Downdrafts Associated with a Squall Line

J. SUN, S. BRAUN, M. I. BIGGERSTAFF,* R. G. FOVELL,** AND R. A. HOUZE, JR.

Department of Atmospheric Sciences, University of Washington, Seattle, Washington

21 September 1992 and 25 March 1993

ABSTRACT

Thermodynamic retrieval analysis applied to a composite of dual-Doppler radar data obtained in the 10–11 June 1985 PRE-STORM (Preliminary Regional Experiment for STORM-Central) squall line and a model simulation of a similar squall line show that the upper-level downdrafts located ahead of and behind the main convective updraft zone were generally positively buoyant. As a result, the upper-level downdrafts contributed negatively to the system heat flux.

1. Introduction

The squall line with a trailing stratiform region is a type of mesoscale convective system that occurs both in the tropics and midlatitudes. The distinctive organization and longevity of this type of storm have made it an attractive subject for intensive study (e.g., Zipser 1969, 1977; Houze 1977). In addition to the importance of these storms themselves, the understanding of the relatively simple structure of the squall line should provide insight into other more complicated convective systems. Houze et al. (1990) found that while only a few springtime storms in Oklahoma are of the purely leading line–trailing stratiform type, two-thirds of all mesoscale convective systems in that environment exhibit some degree of this type of organization.

Although the circulation, thermodynamics, cloud microphysics, and precipitation structure of the squall line with a trailing stratiform region have been documented to a considerable degree, there remain key features that need to be clarified. The purpose of this note is to address one particular feature—the upper-level downdrafts that occur in association with these squall lines.

The squall line with trailing stratiform precipitation is typically characterized by a line of heavy precipitation, called the "convective region," followed by a lighter more uniform precipitation area referred to as the "stratiform region." The stratiform region can be further subdivided according to the low-level radar reflectivity structure. Immediately behind the convective region is the transition zone, which is usually identifiable as a relative minimum in reflectivity at mid- to low levels. The transition zone was first described by Ligda (1956), and subsequently by many other investigators (Smull and Houze 1985; Chong et al. 1987; Rutledge et al. 1988; Houze et al. 1990; Biggerstaff and Houze 1991a, 1991b, 1993). It marks the beginning of the trailing stratiform precipitation region. Just behind the transition zone, in the center of the stratiform region, is a secondary maximum in radar reflectivity and rainfall rate. The precipitation in this band is not as intense as in the leading convective line; it is much more uniform in intensity, and it is located beneath a well-defined radar bright band at the melting level. The precipitation structure associated with the squall line with trailing stratiform precipitation is described further by Houze et al. (1989, 1990).

Some of the upper-level downdrafts associated with a squall-line system occur just ahead of the convective region (Hoxit et al. 1976). It is thought that the subsidence in these drafts is characterized by adiabatic warming, and that presquall low pressure areas are associated with this warming (Fritsch and Chappell 1980). Immediately to the rear of the presquall upper-level downdrafts are the main deep updrafts of the convective region. Additional upper-level downdrafts are found behind the updrafts. Sometimes they are located in the rear part of the convective region (Heymsfield and Schotz 1985; Smull and Houze 1987a). In other cases, they are found within the transition zone (Biggerstaff and Houze 1991a, 1993).

From the standpoint of large-scale heating, the thermal structures of these downdrafts are important. Following Houze (1982, 1989), the mesoscale system vertical heat flux can be written as

* Current affiliation: Department of Meteorology, Texas A&M University, College Station, Texas.

** Current affiliation: Department of Atmospheric Sciences, University of California, Los Angeles, California.

Corresponding author address: Scott Braun, Department of Atmospheric Sciences, AK-40, University of Washington, Seattle, WA 98195.

$$\sigma_c M_c(s_c - s_e) = \sigma_{cu} M_{cu}(s_{cu} - s_e) + \sigma_{cd} M_{cd}(s_{cd} - s_e), \quad (1)$$

where σ_c is the fractional area occupied by cloud, M_c the cloud mass flux, $s = c_p T + gZ$ the dry static energy, c_p the specific heat at constant pressure, T temperature, g gravity, and Z height. The subscripts u, d, and e refer to updrafts, downdrafts, and environmental quantities. From (1), it can be seen that warm updrafts and cold downdrafts contribute positively to the system heat flux, while warm downdrafts contribute negatively to the heat flux.

Little has been determined about the thermodynamics of the upper-level downdrafts in squall-line systems. From the studies of Hoxit et al. (1976) and Fritsch and Chappell (1980), it appears that the downdrafts ahead of the convective line are warm, that is, positively buoyant. Even less is known about the thermal structure of the upper-level downdrafts to the rear of the convective updrafts. Heymsfield and Schotz (1985) speculated that they are composed of air forced downward as a result of the outflow from the tops of the intense updrafts converging with the ambient air at high levels just behind the line of convective updrafts. Smull and Houze (1987a) concurred and suggested that they are thus quite distinct from the downdrafts that originate in mid- to low levels as a result of evaporation, melting, and hydrometeor drag.

Whenever buoyant updrafts arise, the pressure force field associated with the buoyant parcels must push environmental air out of the way. Air near the top of the buoyant parcel moves upward and laterally, while at the base of the parcel air must move in and up to replace the rising buoyant element. Mass continuity requires that the air at the sides of the buoyant element be pushed down. Lilly (1960) and Fritsch (1975) pointed out that the downward motion required by mass continuity in the vicinity of rapidly growing updrafts tends to occur quite close to the intense updrafts. The downward-forced air will rebound, and it has long been suspected that gravity-wave motions occur in the upper troposphere in the vicinity of the tops of the main updrafts (e.g., Figs. 13 and 14 of Palmén and Newton 1969). More recently, Fovell et al. (1992) have presented model results that indicate that the convective updrafts in the leading line of convection produce gravity waves in the upper levels both ahead of and to the rear of the convective line. These interpretations of the downward motions aloft in squall lines are not mutually exclusive, and may indeed just be various ways of saying the same thing. In any case, the ambient air at high levels is most likely stable, and the forced downdrafts would be expected to be positively buoyant, at least in their lower portions. So far, however, this fact has not been confirmed by observation.

In this paper, we cannot report on direct observations of the thermal structure of the upper-level downdrafts. However, we have available to us a detailed composite of the Doppler radar–derived wind field in the 10–11 June 1985 squall line observed during the Oklahoma–Kansas PRE-STORM (Preliminary Regional Experiment for STORM-Central) field project. Biggerstaff and Houze (1991a, 1991b) combined the Doppler radar data with upper-air sounding data in a composite analysis to reconstruct the three-dimensional air circulation inside the mesoscale convective system and in the surrounding environment. In the portion of the composite analysis constructed from the Doppler radar data, the wind field is particularly detailed and shows upper-level downdrafts both ahead of the convective updrafts and to the rear of them in the transition zone. Biggerstaff and Houze (1993) further investigated the region covered by Doppler radar data by constructing a more detailed composite analysis from just the high-resolution dual-Doppler wind fields. The Doppler radar composite is sufficiently detailed that it can be subjected to thermodynamic analysis by the retrieval technique of Hauser et al. (1988). We use this retrieval technique to diagnose the thermal structure of the upper-level downdrafts. At present, this type of diagnosis is the closest we can come to observations of the thermal structure of the upper-level downdrafts.

The following sections describe results based on the retrieval analysis, which confirm that the upper-level downdrafts are nearly neutral or positively buoyant. We also reanalyze the results of the modeling study of Fovell and Ogura (1988), who simulated a squall line similar to the one of 10–11 June 1985. Reexamination of their results shows that the upper-level downdrafts in the model simulation were also positively buoyant. To show the overall consistency as well as limitations of the retrieval analysis, we will present the full fields of retrieved potential temperature perturbation and pressure perturbation in the discussions that follow.

2. The retrieval technique

In this study, we use a thermodynamic and microphysical retrieval technique that closely follows the "dynamic method" of Hauser et al. (1988). Braun and Houze (1993) describe the application of this retrieval method to the 10–11 June 1985 squall line. This technique diagnoses potential temperature and pressure perturbations, defined with respect to an undisturbed environment or "base state," as well as mixing ratios for rain, precipitation ice, cloud water, cloud ice, and water vapor. The wind field, synthesized from Doppler radar observations, is assumed to be given. The Doppler winds are used to estimate the horizontal and vertical advection of the vertical and horizontal components of the wind. The retrieved microphysical variables are used to help estimate the latent heating rates. With these inputs, the vertical and horizontal equations of motion and thermodynamic equation are solved si-

multaneously. A variational approach is used[1] in which the perturbation fields of pressure and potential temperature that are statistically most consistent with the observed wind and precipitation fields are sought. Both the horizontal and vertical gradients of the potential temperature and pressure are derived in the variational analysis. Thus, this is not a retrieval where an unknown constant at each level is missing, as was the case in some earlier types of retrieval techniques.

A thermodynamic retrieval technique similar to that used here was recently tested by Sun and Houze (1992). They used the output of Fovell and Ogura's (1988) numerical simulation of a squall line with trailing stratiform precipitation. Application of the retrieval to the time-averaged wind and radar reflectivity fields of the model, for which the time changes of the mean variables were nil, showed that the thermodynamics of the stratiform region were generally well reproduced. However, significant errors resulted in the convective region, because eddy correlations of the temporally fluctuating wind fields (i.e., $\overline{u'w'}$, where the prime denotes a deviation from the time average value, indicated by the overbar) in the convective region were not taken into account in the retrieval. Application of the retrieval to the instantaneous model wind fields indicated that very high radar scan rates would be required in a real case in order to estimate accurately local time derivatives or to assure good retrieval results in parts of the storm where time changes are large and nonlinear.

In the real case examined below, the mean time changes over the time period of the composite storm are not exactly zero. As a consequence, when we perform the retrieval on mean composite wind fields, the absence of both eddy flux terms and time change terms contributes to errors. Hence, although the validation work of Sun and Houze (1992) gives us some confidence to apply the retrieval to the stratiform region, the results presented below should be viewed with caution. Matejka (1989) has indeed shown that the thermodynamic perturbations in the stratiform region of the 10–11 June 1985 PRE-STORM squall line were not fully explained by the steady component of the radar-observed wind fields. Since the composite dataset used here was constructed under the steady-state assumption, the evolutionary component cannot be resolved in the present retrieval. Furthermore, because of the compositing of the dual-Doppler synthesized wind fields, smoothing of the small-scale wind features leads to smoothing of small-scale features in the retrieved fields. However, for our limited objective, which is simply to indicate the sign and general magnitude of the thermodynamic perturbations in the upper-level downdrafts, the present technique provides very suggestive, though not conclusive, evidence for the warm nature of the upper-level downdrafts.

The retrieval results obtained here are presented in a single x–z vertical cross-sectional plane. The two-dimensional framework is adopted to minimize the computational time, which is considerable for two-dimensional calculations and significantly greater for three-dimensional calculations. The governing equations for the thermodynamic retrieval are adapted to the two-dimensional framework by taking their along-line (Y) averages. Therefore, the equations include terms involving the Y mean variables ($\bar{u}$, $\bar{v}$, $\bar{w}$, etc., where the overbar here represents a Y average) as well as the deviations from the Y mean (u'', v'', w'', etc.). To simplify the analysis further, we assume that the deviations from the along-line mean for potential temperature and the microphysical variables are negligible. The two-dimensional framework is a limitation of the present analysis, but the results appear adequate for our limited objectives.

3. Data and environment

The 10–11 June 1985 squall line reached the mature stage soon after it entered the PRE-STORM observation network in Kansas and Oklahoma. This network contained densely spaced surface and upper-air sounding stations and two pairs of Doppler radars: one pair in Oklahoma and the other in Kansas (Cunning 1986). The data used in this study are from the Doppler radar pair in Kansas, where two 5-cm-wavelength Doppler radars (the CP-3 and CP-4 radars of the National Center for Atmospheric Research) were operated near Wichita. Coordinated dual-Doppler scans were obtained with these radars at 0139, 0209, 0220, 0345, 0414, and 0510 UTC 11 June 1985. However, none of these scans covered the entire storm since the quantitative radar range of each radar was only 135 km, and the area of dual-Doppler coverage was much smaller than the area scanned by each radar alone.

To obtain coverage across the whole storm, a composite was constructed using the dual-Doppler data from each of the foregoing coordinated scans. The composite was constructed by placing winds from each of the individual dual-Doppler syntheses, for different times and locations, into a coordinate system attached to the moving storm by assuming the storm had a steady structure during this time period and moved with a speed of 14 m s^{-1} from the west-northwest (300°). The composite three-dimensional wind and reflectivity fields covered most of the northern portion of the radar reflectivity pattern in Fig. 1. [See Fig. 6e of Biggerstaff and Houze (1991a) for the exact area covered.] A 60-km × 360-km rectangular subregion of the radar data composite (outlined by the rectangle in

[1] The variational method of Roux and Sun (1990) is used instead of that described in Hauser et al. (1988). Sun and Houze (1992) showed that the Roux and Sun (1990) variational method works well within the stratiform precipitation region.

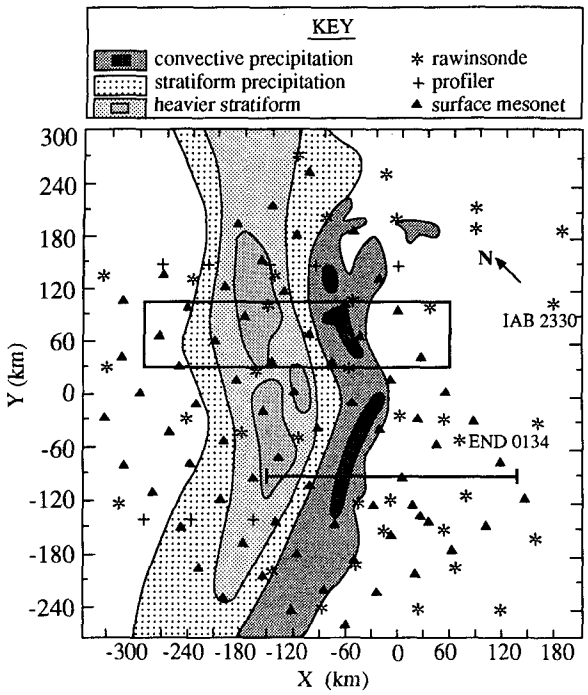

FIG. 1. Map showing the 10–11 June 1985 PRE-STORM squall line system in the composite coordinate system of Biggerstaff and Houze (1991a). The locations of the convective, stratiform, and heavier stratiform precipitation are indicated by shading. The region for which the thermodynamic retrieval analysis was carried out is outlined by the rectangle. Locations of rawinsonde soundings, profiler soundings, and surface stations are indicated. IAB 2330 and END 0134 identify the two rawinsonde soundings referred to in the text. The surface mesonet soundings operated continuously, and the bar attached to one of the stations indicates the length of the record of data that was obtained at each station during the period of the composite.

Fig. 1) was selected for the thermodynamic retrieval because this portion of the storm exhibited the most nearly two-dimensional structure. The horizontal and vertical resolutions of the composite wind fields are 3 and 0.5 km, respectively.

Since PRE-STORM had a fairly dense upper-air sounding network, there were several soundings taken on which one could base the environment used in the retrieval analysis. At 2330 UTC, the station IAB (McConnell Air Force Base) was located directly ahead of the squall-line area (Fig. 1), and the relative wind at the surface into our study area was from that direction. However, the sounding launched from IAB at 2330 UTC was not especially close to the squall line, and it showed a very stable troposphere. The convective available potential energy (CAPE; Moncrieff and Miller 1976) was only 62 $m^2 s^{-2}$, and the convective inhibition (CIN; Colby 1983; Bluestein and Jain 1985) was -251 $m^2 s^{-2}$. Other soundings located in the upper right part of Fig. 1 were similar. This region of stability was produced by earlier mesoscale convective activity. A squall line could not be maintained in that environment, and Rutledge et al. (1988) reported that the convective line decayed as it moved into this area.

The soundings located in the lower right part of the mesonet area had much higher CAPE and generally weaker CIN. As such, they were more representative of the air feeding the active squall line. At the surface, the trajectories extending from Enid, Oklahoma, (END, Fig. 2) reached the bowed-out part of the con-

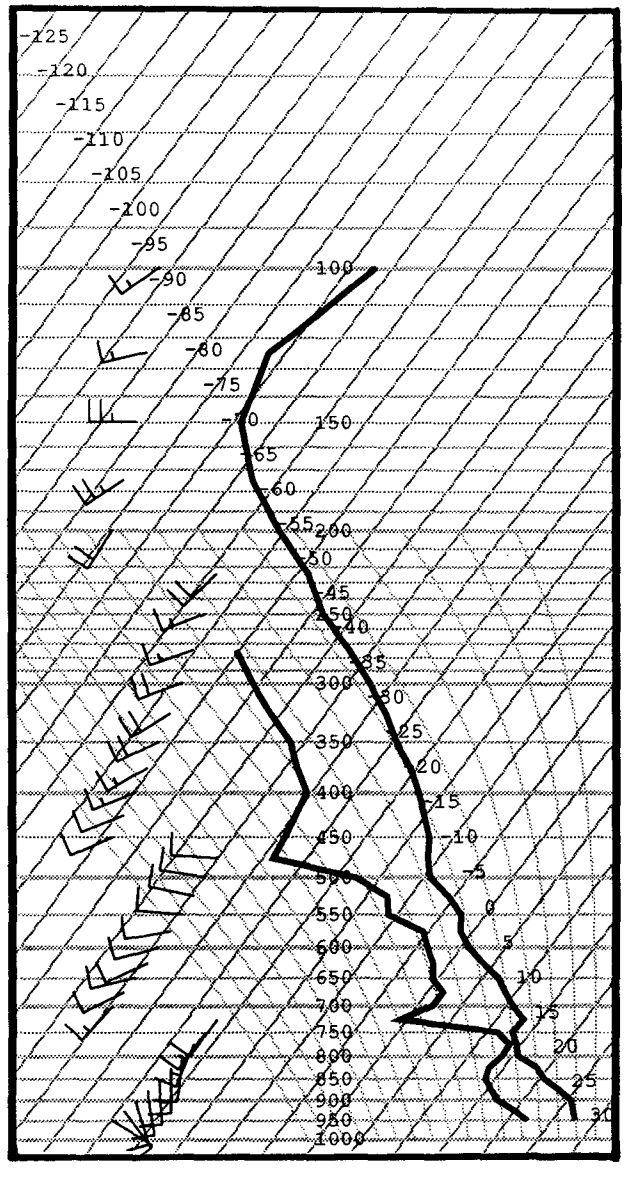

FIG. 2. Skew T-log$p$ diagram of rawinsonde data obtained at Enid, Oklahoma, at 0134 UTC 11 June 1985. Temperature (sloping lines) is labeled in degrees Celsius. Pressure levels are labeled in millibars. Curved reference lines are moist adiabats. Winds are plotted in standard format, with one full flag corresponding to 5 m s^{-1}. The flags are staggered to minimize overlap in plotting.

vective line just south of the analysis domain, while at 800 mb, the trajectories extended into the analysis domain (see Biggerstaff and Houze 1991a, Fig. 14a). The sounding launched at 0134 UTC at station END is therefore used to represent the undisturbed base state. The moist adiabat determined from the lowest 500-m layer is characterized by a wet-bulb potential temperature of 25°C, the CAPE is 2035 $m^2 s^{-2}$, the CIN is 52 $m^2 s^{-2}$, and the equilibrium temperature level for a parcel lifted from low levels is at about 14.5 km. These parameters characterize an atmosphere in which deep convection could be maintained.

4. Composite reflectivity and wind fields

The composite vertical cross sections of reflectivity (Fig. 3a) and wind components (Figs. 3b–d) exhibit features typical of a mature squall line with a region of trailing stratiform precipitation. In this section we review these basic fields. The clear and consistent structure of these fields is the foundation for the retrieval analysis described in section 5.

The composite radar reflectivity field (Fig. 3a) indicates that the leading convective region is roughly 60 km wide and contains a maximum of nearly 45 dBZ at $X = -50$ km. The 37.5-dBZ contour reaches the 7.5-km level, while the 22.5-dBZ contour reaches 13 km. The deep convection is consistent with the high equilibrium temperature level (14.5 km) of the END 0134 UTC sounding. Behind the convective region, the 22.5-dBZ contour drops to 5.5-km altitude, and like others, it maintains nearly the same altitude across the 150-km-wide stratiform region. The transition zone, identified as a relative minimum of radar reflectivity at low levels, is located between the convective and stratiform regions, centered at $X = -85$ km.

Front-to-rear relative flow (negative u velocity) extends up to 9.5 km at the front edge of the convective line, rises within the convective region, and continues throughout the trailing stratiform region at mid- to upper levels (Fig. 3b). Front-to-rear flow is also found at low levels, where it increases in strength toward the rear of the storm. A layer of rear-to-front flow (positive u velocity) slopes from midlevels at the back edge of the stratiform region, where it is maximum, to low levels in the convective region. This feature is the "rear-inflow jet" (Smull and Houze 1987b; Rutledge et al. 1988; Houze et al. 1989). A rear-to-front flow also appears at the leading edge of the storm at upper levels. This upper-level rear-to-front air motion is sometimes referred to as "overturning" flow (Moncrieff 1978).

The along-line velocity component (v, Fig. 3c) has the same magnitude as the cross-line flow and is especially strong at high levels, where it exceeds 25 m s^{-1}. "Southerly" flow (i.e., positive v velocity) extends from the front of the convective line up through the convective region and across the trailing stratiform region at mid- to upper levels. "Northerly" flow (negative v velocity) was observed at mid- to low levels from the back of the system to near the front of the convective line.

The vertical velocity field (w, Fig. 3d) also exhibits features typical of squall lines with trailing stratiform precipitation. In the leading convective region of the storm, the vertical velocity field (Fig. 3d) consisted of

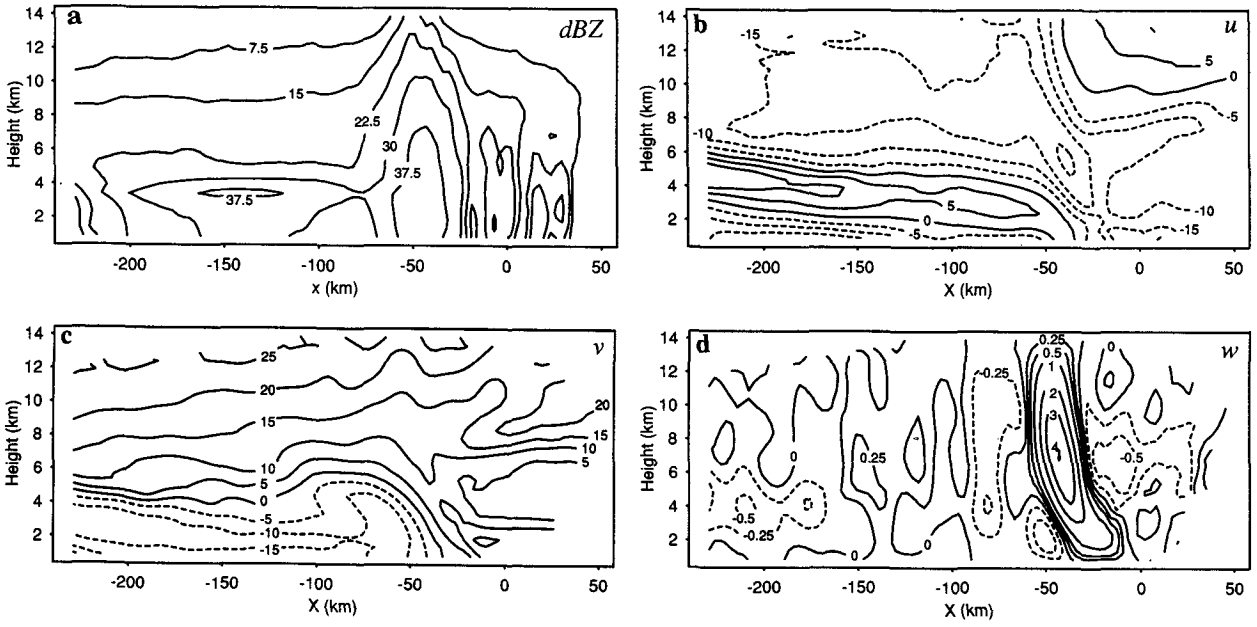

FIG. 3. Along-line averaged composite vertical cross-sectional fields of (a) radar reflectivity (dBZ); (b) system-relative line-normal horizontal wind velocity component (m s^{-1}); (c) along-line wind velocity component (m s^{-1}); and (d) vertical velocity component (m s^{-1}).

upward motion on average, with a maximum value of 4 m s^{-1} at the 7-km level. In the stratiform region, downward air motion occurred across most of the storm at lower levels, in the manner described by Zipser (1969, 1977) and Houze (1977). An enhanced region of subsidence occurred at the rear of the stratiform region, where it helped establish a "wake low" at the back edge of the rain area (as described by Johnson and Hamilton 1988). A mesoscale updraft is found in the trailing stratiform region in mid- to upper levels, above the mesoscale downdraft, as is typical of nearly all mesoscale convective systems (Houze 1989).

Smaller-scale downdrafts are found just ahead, immediately behind, and within the convective region of the storm. Lower-tropospheric convective downdrafts, likely driven by precipitation loading and evaporation, account for the mean descent at low levels near $X = -50$ km in Fig. 3d. Mid- to upper-level mean downward motion was found both ahead of the convective updraft zone, where it was likely responsible for the presquall mesolow, as discussed in Biggerstaff and Houze (1991a), and in the transition zone behind the convective updraft (between $X = -65$ and -90 km), where the subsidence extended from the storm top to the ground.

The deep subsidence in the transition zone has separate peaks of downward motion, at $Z = 4$ and 10 km. The separate peaks of downward motion in this zone indicate that the column of downward motion is produced by two separate processes. Biggerstaff and Houze (1993) suggest that this column of downdraft was not a continuous feature transporting near-tropopause air down to the surface, but rather that the deep subsidence was the result of a vertical alignment of lower- and upper-level downdrafts produced by different mechanisms. *It is the upper-level downdraft in this column as well as the mid- to upper-level downward motion just ahead of the convective updraft zone that are the features whose thermal structure we seek in this paper.*

As discussed by Fovell and Ogura (1988) and Biggerstaff and Houze (1993), the mean upper-level downdraft defined by the mean downward motion in the transition zone was the average effect of smaller-scale downdrafts originating in the convective region and moving front to rear across the transition zone. These smaller building blocks of the mean upper-level downdraft, for reasons discussed by Sun and Houze (1992), were not sufficiently resolved in time by the PRE-STORM radar observations to be candidates for the retrieval analysis. Hence, we can apply the retrieval only to the mean composite fields shown in Fig. 3.

5. Retrieved thermodynamic fields

a. Thermal perturbations

The retrieved potential temperature perturbations θ' for the 10–11 June 1985 squall line are shown in Fig. 4a. Positive values are found at levels from roughly 4–12 km all across the squall line, with maximum values exceeding 3 K within and slightly rearward of the convective updraft near the 6-km level. The warm air aloft generally became less buoyant with increasing distance from the convective region. Negative values are found below 4 km, with perturbations less than -6 K near the surface in the vicinity of the convective downdraft. Negative perturbations are also seen above 12 km.

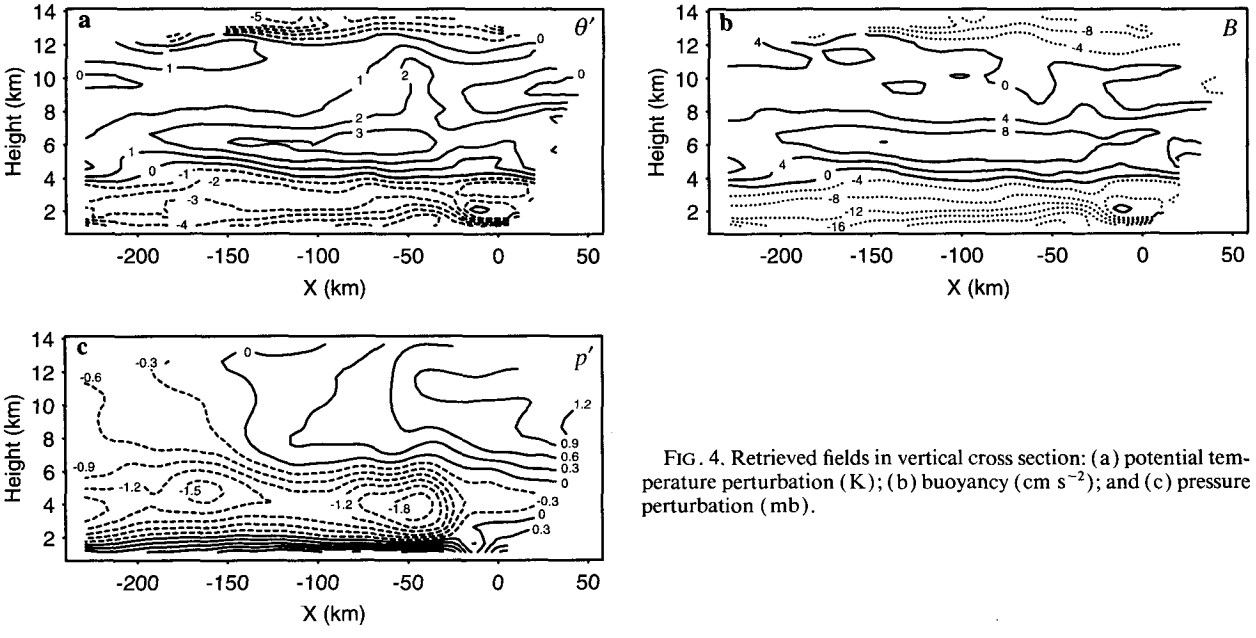

FIG. 4. Retrieved fields in vertical cross section: (a) potential temperature perturbation (K); (b) buoyancy (cm s^{-2}); and (c) pressure perturbation (mb).

We define the total buoyancy as

$$B = g\left(\frac{\theta'}{\theta_0} - \frac{p'}{p_0} + 0.61q'_v - q_H\right), \qquad (2)$$

where θ is the potential temperature, p pressure, q_v the water vapor mixing ratio, and q_H the total hydrometeor mixing ratio. Primed quantities represent deviations from an assumed mean environmental state (taken as the Enid sounding and indicated by the subscript 0). Thus, when we refer to a region within the squall line as positively buoyant, we mean that the region is buoyant with respect to the mean environment. We do not imply that a parcel is necessarily more buoyant than immediately adjacent parcels. Given this definition of buoyancy, B is computed from the retrieved potential temperature, pressure (discussed in section 5b), and microphysical variables (not shown). The resultant buoyancy field is shown in Fig. 4b.

From these results, it is evident that the region of upper-level downdrafts located between the convective updraft and mesoscale updraft zones (between $X = -65$ and -90 km) was positively buoyant on average in the 4–9.0-km altitude range and near neutral (or slightly negative) between 9.0- and 12-km altitude (compare Fig. 3d and Fig. 4b). Between 4 and 9.0 km, the mean buoyancy in the upper-level downdrafts of the transition zone differs only slightly from the positive buoyancy of the neighboring updraft zones. In fact, the region of slightly negative buoyancy between $X = -5$ and -80 km and $Z = 9$ and 12 km is located in the rear part of the convective updraft and the forward part of the transition zone downdraft. In the rear part of the transition zone downdraft ($X = -80$ to -90 km), the buoyancy is slightly positive. These findings are consistent with gravity-wave motion. Similarly, it is evident that the upper-level downdrafts ahead of the main convective updraft zone were positively buoyant on average. *This indication by the retrieval technique, that the upper-level downdrafts are generally positively buoyant, is the main result of this study.* Furthermore, the finding that the downdrafts aloft are warm implies that the vertical heat fluxes associated with the downdrafts ahead of and behind the convective updraft are negative, in contrast to the positive vertical heat flux associated with the negatively buoyant downdrafts at lower levels. These conclusions, however, are based on the thermodynamic structure of the mean upper-level downdrafts. With the available data, we cannot show that individual, more intense downdrafts at a given time are also warm.

b. *Pressure perturbations*

Confidence in the reliability of the retrieved thermal perturbation fields is gained by examining the pressure perturbation field p', which is diagnosed from the radar data simultaneously with the thermal perturbation field (Fig. 4c). In particular, the surface pressure pattern can be inspected for consistency with the pressure field indicated independently by the surface and sounding mesonetwork of PRE-STORM (Cunning 1986).

The generally high pressure at low levels is related hydrostatically to the cold thermal perturbation that prevails throughout low levels (Fig. 4a). In Fig. 4c, the magnitude of the pressure perturbation seen at the lowest level of the analysis (1140 m) decreases gradually toward the rear of the storm. This gradient is consistent with the surface pressure pattern deduced from the mesonet data by Johnson and Hamilton (1988) and Biggerstaff and Houze (1991a). These investigators found a wake low at the surface located at the back edge of the rain area. Sounding data described by Johnson and Hamilton (1988) confirm that the wake low was hydrostatically related to the thermal perturbation field. A maximum of warming (as seen in our retrieval at about $X = -225$ km and $Z = 4$–5 km) and drying was found directly above the wake low. This interpretation is consistent with Figs. 3a, 3b, and 3d, in which strong descent is seen in association with the rear-inflow jet at the back edge of the stratiform precipitation region. Apparently, as suggested by Johnson and Hamilton (1988), hydrometeors in that area were being evaporated or sublimated rather quickly, and with the strong descent in that location, the evaporative cooling was not able to counter the subsidence warming, and a wake low was produced.

The retrieved pressure perturbation at low levels also decreases toward the leading edge of the storm. In Fig. 4c, it is seen to decrease with increasing X from $X = -30$ to -10 km, that is, from the heaviest rainfall area outward toward the leading edge of the storm. The lowest pressures ($X \approx -15$ km) occur just ahead of the leading convective line (see Fig. 3a) and beneath the strong midlevel descent ahead of the convective updraft (Fig. 3d). This minimum in pressure apparently results from the relatively warm pocket of air at $X = -10$ km, $Z = 2$ km in Fig. 4a. Biggerstaff and Houze (1991a) found evidence of a presquall low in the surface mesonet data, just ahead of the surface rainfall (see their Fig. 15d).

6. Comparison with previous studies

a. *Previous retrieval studies*

To our knowledge, no previous retrieval studies have indicated the thermal structure of the upper-level downdrafts of a squall line with trailing stratiform precipitation. An upper-level downdraft was found in the composite transition zone of a West African squall line (see Fig. 6d of Chalon et al. 1988). However, thermodynamic retrieval analyses performed on this case did not encompass the upper-level downdraft (Roux 1988; Sun and Roux 1988).

b. Thermal structure of upper-level downdrafts shown by models

A numerical simulation of the West African squall line described and analyzed by Chalon et al. (1988), Roux (1988), and Sun and Roux (1988) has been carried out by Lafore and Moncrieff (1989). Although Lafore and Moncrieff do not explicitly address the thermodynamics of upper-level downdrafts, comparison of their Figs. 8 and 15 indicates that downdrafts behind the convective region were positively buoyant between the 4- and 8-km levels.

Fovell and Ogura (1988) simulated an Oklahoma squall line that had characteristics rather similar to the 10–11 June 1985 PRE-STORM case studied here. Their study also did not address the buoyancy of the upper-level downdrafts. Model output data from their simulation is replotted in Fig. 5, with a set of contour intervals in Fig. 5a that more clearly indicate the updrafts and downdrafts of the storm. The results of this simulation clearly show that positive buoyancy characterized the downdrafts just behind the convective updraft (compare Figs. 5a and 5b).

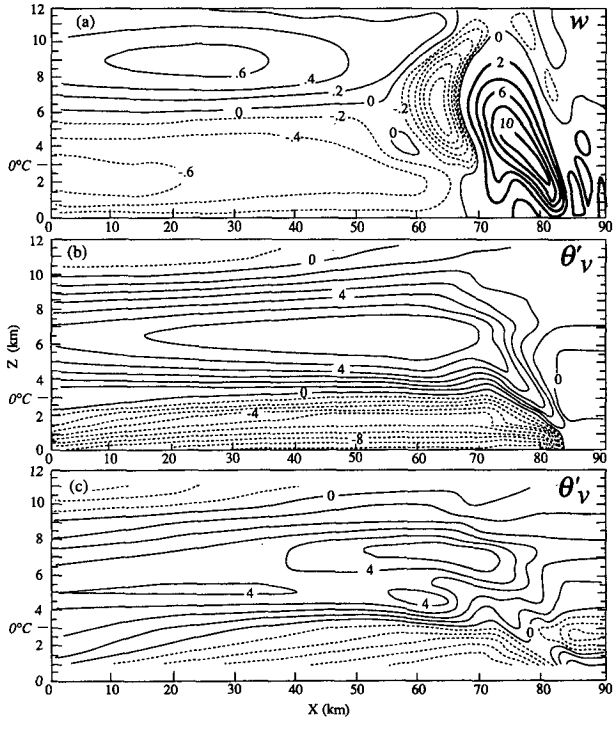

FIG. 5. Time-averaged fields from Fovell and Ogura's (1988) model simulation of the 22 May 1976 Oklahoma squall line. (a) Two types of contours are used to show the vertical velocity component. In the convective updraft region darker contours are used. The contour interval is 2 m s^{-1}. Elsewhere, thinner lines are used at 0.2 m s^{-1} intervals. This scheme allows both the intense convective upward motion and the less intense vertical velocity features to be seen clearly in the same diagram. Negative (downward) vertical velocities are indicated by dashed contours. (b) Cloud virtual potential temperature perturbation (K). (c) Cloud virtual potential temperature perturbation (K) obtained by Sun and Houze (1992) by applying the retrieval technique of Roux and Sun (1990) to a time average of Fovell and Ogura's (1988) model results.

To determine how the upper-level downdrafts in the model simulation of Fovell and Ogura (1988) would appear in a retrieval analysis of the type we have applied to the 10–11 June 1985 PRE-STORM case, the retrieval technique has been applied to the time-averaged model wind and reflectivity fields (Sun and Houze 1992). The virtual potential temperature perturbation θ'_v diagnosed from the model output is shown in Fig. 5c. Although not as smooth as the model thermal perturbation field, the buoyancy retrieved from the model output is again clearly positive across the region of the downdraft (compare Figs. 5a and 5c).

7. Conclusions

A thermodynamic retrieval technique applied to a composite of the wind and reflectivity fields of the 10–11 June 1985 squall line observed by dual-Doppler radar during PRE-STORM indicates that the upper-level downdrafts ahead of and behind the intense convective updrafts of the leading line were positively buoyant in the 4–9.5-km altitude range. The thermal buoyancy of these averaged downdrafts is nearly indistinguishable from that of the neighboring averaged updrafts. On average, the downdrafts at these levels thus contribute negatively to the vertical heat flux by the mesoscale system.

Confidence in these results is gained from the quality of the composite radar dataset and the consistency of the various observed and derived fields. The radar data contain the essential features of a squall line with trailing stratiform precipitation: the leading line of intense convective rain, the reflectivity trough or transition zone immediately following the convective band, the trailing stratiform precipitation with its secondary maximum of surface rain rate beyond the transition zone, and the rear-inflow jet in midlevels through the stratiform region with front-to-rear flows above and below. The vertical velocity field derived from the dual-Doppler winds is reasonably consistent with the two-dimensional nonhydrostatic model simulation of a similar squall line by Fovell and Ogura (1988), as well as other similar modeling studies. The retrieved pressure perturbation field appears consistent with the PRE-STORM surface and upper-air data, which show a wake low behind and a presquall low ahead of the storm.

The results of this study confirm the expectation stated in the Introduction. The upper-level downdrafts both ahead and behind the main updraft zone of the convective line consist of air forced downward below its equilibrium level. As such, they owe their existence to a physical cause that is quite distinct from the origin of the lower-altitude downdrafts, which are negatively buoyant and brought on by precipitation loading and the cooling effects of evaporation and melting. Oddly, though, as was seen in Fig. 3d, and as has been pointed out by Biggerstaff and Houze (1993), there is a tendency for the upper-level, positively buoyant down-

drafts to overlie the lower-level negatively buoyant downdrafts in the transition zone, giving the latter the characteristic of being a deep column of downward motion on average. Whether this vertical alignment of different types of downdrafts is endemic to this type of squall line or rather a peculiar characteristic of the 10–11 June 1985 PRE-STORM squall line is a question that begs further investigation.

Acknowledgments. Some of the software for the retrieval was supplied by Dr. Frank Roux. G. C. Gudmundson edited the manuscript and K. M. Dewar drafted some of the figures. This work was supported by the National Science Foundation under Grant ATM9101653.

REFERENCES

Biggerstaff, M. I., and R. A. Houze, Jr., 1991a: Kinematic and precipitation structure of the 10–11 June 1985 squall line. *Mon. Wea. Rev.*, **119**, 3034–3065.

——, and ——, 1991b: Midlevel vorticity structure of the 10–11 June 1985 squall line. *Mon. Wea. Rev.*, **119**, 3066–3079.

——, and ——, 1993: Kinematics and microphysics of the transition zone of the 10–11 June 1985 squall line. *J. Atmos. Sci.*, **50**, 3091–3110.

Bluestein, H. B., and M. H. Jain, 1985: Formation of mesoscale lines of precipitation: Severe squall lines in Oklahoma during the spring. *J. Atmos. Sci.*, **42**, 1711–1732.

Braun, S. A., and R. A. Houze, Jr., 1993: The transition zone and secondary maximum of radar reflectivity behind a midlatitude squall line: Results retrieved from Doppler radar data. *J. Atmos. Sci.*, submitted.

Chalon, J. P., G. Jaubert, F. Roux, and J. P. Lafore, 1988: The West African squall line observed on 23 June 1981 during COPT 81: Mesoscale structure and transports. *J. Atmos. Sci.*, **45**, 2744–2763.

Chong, M., P. Amayenc, G. Scialom, and J. Testud, 1987: A tropical squall line observed during the COPT 81 experiment in West Africa. Part I: Kinematic structure inferred from dual-Doppler radar data. *Mon. Wea. Rev.*, **115**, 670–694.

Colby, F. P., Jr., 1983: Convective instability as a predictor of convection during AVE-SESAME II. *Mon. Wea. Rev.*, **112**, 2239–2252.

Cunning, J. B., 1986: The Oklahoma–Kansas Preliminary Regional Experiment for STORM-Central. *Bull. Amer. Meteor. Soc.*, **67**, 1478–1486.

Fovell, R. G., and Y. Ogura, 1988: Numerical simulation of a midlatitude squall line in two dimensions. *J. Atmos. Sci.*, **45**, 3846–3879.

——, D. R. Durran, and J. R. Holton, 1992: Numerical simulations of convectively generated gravity waves in the atmosphere. *J. Atmos. Sci.*, **49**, 1427–1442.

Fritsch, J. M., 1975: Cumulus dynamics: Local compensating subsidence and its implications for cumulus parameterization. *Pure Appl. Geophys.*, **113**, 851–867.

——, and C. F. Chappell, 1980: Numerical prediction of convectively driven mesoscale pressure systems. II: Mesoscale model. *J. Atmos. Sci.*, **37**, 1734–1762.

Hauser, D., F. Roux, and P. Amayenc, 1988: Comparison of two methods for the retrieval of thermodynamic and microphysical variables from Doppler-radar measurements: Application to the case of a tropical squall line. *J. Atmos. Sci.*, **45**, 1285–1303.

Heymsfield, G. M., and S. Schotz, 1985: Structure and evolution of a severe squall line over Oklahoma. *Mon. Wea. Rev.*, **113**, 1563–1589.

Houze, R. A., Jr., 1977: Structure and dynamics of a tropical squall-line system. *Mon. Wea. Rev.*, **105**, 1540–1567.

——, 1982: Cloud clusters and large-scale vertical motions in the tropics. *J. Meteor. Soc. Japan*, **60**, 396–410.

——, 1989: Observed structure of mesoscale convective systems and implications for large-scale heating. *Quart. J. Roy. Meteor. Soc.*, **115**, 425–461.

——, B. F. Smull, and P. Dodge, 1990: Mesoscale organization of springtime rainstorms in Oklahoma. *Mon. Wea. Rev.*, **118**, 613–654.

——, S. A. Rutledge, M. I. Biggerstaff, and B. F. Smull, 1989: Interpretation of Doppler weather radar displays of midlatitude mesoscale convective systems. *Bull. Amer. Meteor. Soc.*, **70**, 608–619.

Hoxit, L. R., C. F. Chappell, and J. M. Fritsch, 1976: Formation of mesolows or pressure troughs in advance of cumulonimbus clouds. *Mon. Wea. Rev.*, **104**, 1419–1428.

Johnson, R. H., and P. J. Hamilton, 1988: The relationship of surface pressure features to precipitation and airflow structure of an intense midlatitude squall line. *Mon. Wea. Rev.*, **116**, 1444–1472.

Lafore, J. P., and M. W. Moncrieff, 1989: A numerical investigation of the organization and interaction of the convective and stratiform regions of tropical squall lines. *J. Atmos. Sci.*, **46**, 521–544.

Ligda, M. G. H., 1956: The radar observations of mature prefrontal squall lines in the midwestern United States. *Sixth Congress of Organization Scientifique et Technique International du Vol a Voile (OSTIV)*, Fédération Aéronautique Internationale, St-Yan, France, publication, **4**, 1–3.

Lilly, D. K., 1960: On the theory of disturbances in a conditionally unstable atmosphere. *Mon. Wea. Rev.*, **88**, 1–17.

Matejka, T., 1989: Pressure and buoyancy forces and tendencies in a squall line and their relation to its evolution. Preprints, *24th Radar Meteor. Conf.*, Tallahassee, Amer. Meteor. Soc., 478–481.

Moncrieff, M. W., 1978: The dynamical structure of two-dimensional steady convection in constant vertical shear. *Quart. J. Roy. Meteor. Soc.*, **104**, 543–568.

——, and M. M. Miller, 1976: The dynamics and simulation of tropical squall lines. *Quart. J. Roy. Meteor. Soc.*, **102**, 373–394.

Palmén, E., and C. W. Newton, 1969: *Atmospheric Circulation Systems: Their Structure and Physical Interpretation.* Academic Press, 603 pp.

Roux, F., 1988: The West African squall line observed on 23 June 1981 during COPT 81: Kinematics and thermodynamics of the convective region. *J. Atmos. Sci.*, **45**, 406–426.

——, and J. Sun, 1990: Single Doppler observations of a West African squall line on 27–28 May 1981 during COPT81: Kinematics, thermodynamics, and water budget. *Mon. Wea. Rev.*, **118**, 1826–1854.

Rutledge, S. A., R. A. Houze, Jr., M. I. Biggerstaff, and T. J. Matejka, 1988: The Oklahoma–Kansas mesoscale convective system of 10–11 June 1985: Precipitation structure and single Doppler-radar analysis. *Mon. Wea. Rev.*, **116**, 1409–1430.

Smull, B. F., and R. A. Houze, Jr., 1985: A midlatitude squall line with a trailing region of stratiform rain: Radar and satellite observations. *Mon. Wea. Rev.*, **113**, 117–133.

——, and ——, 1987a: Dual-Doppler radar analysis of a midlatitude squall line with a trailing region of stratiform rain. *J. Atmos. Sci.*, **44**, 2128–2148.

——, and ——, 1987b: Rear inflow in squall lines with trailing stratiform precipitation. *Mon. Wea. Rev.*, **115**, 2128–2148.

Sun, J., and F. Roux, 1988: Thermodynamic structure of the trailing stratiform regions of two West African squall lines. *Ann. Geophys.*, **6**, 659–670.

——, and R. A. Houze, Jr., 1992: Validation of a thermodynamic retrieval technique by application to a simulated squall line with trailing stratiform precipitation. *Mon. Wea. Rev.*, **120**, 1003–1018.

Zipser, E. J., 1969: The role of organized unsaturated convective downdrafts in the structure and rapid decay of an equatorial disturbance. *J. Appl. Meteor.*, **8**, 799–814.

——, 1977: Mesoscale and convective scale downdrafts as distinct components of squall line circulation. *Mon. Wea. Rev.*, **105**, 1568–1589.

PAPERS TO APPEAR IN FORTHCOMING ISSUES

ARTICLES

Comparison of Space and Time Errors in Spectral Numerical Solutions of the Global Shallow-Water Equations—MICHAEL J. NAUGHTON, Bureau of Meteorology Research Centre, Melbourne, Victoria, Australia; GERALD L. BROWNING, Cooperative Institute for Research in the Atmosphere, Fort Collins, Colorado; AND WILLIAM BOURKE, Bureau of Meteorology Research Centre, Melbourne, Victoria, Australia.

Dynamics of Short-Term Univariate Forecast Error Covariances—STEPHEN E. COHN, Laboratory for Atmospheres, NASA/Goddard Space Flight Center, Greenbelt, Maryland.

Aircraft Observation of Convection Waves over Southern Germany—A Case Study—THOMAS HAUF, DLR Institut für Physik der Atmosphäre, Oberpfaffenhofen, Germany.

Computing The Horizontal Pressure Gradient Force in Sigma Coordinates—MAURICE DANARD, QING ZHANG, AND JOHN KOZLOWSKI, Department of Computer Science, University of Victoria, Victoria, British Columbia, Canada.

Representation of Clouds in Large-Scale Models—M. TIEDTKE, ECMWF, Reading, Berkshire, England.

A Simple Numerical Method for Hydrostatic Incompressible Models with Rigid Lids—VALDIR INNOCENTINI, NIVALDO SILVEIRA FERREIRA, AND ERNESTO DOS SANTOS CAETANO NETO, Instituto Nacional de Pesquisas Espaciais, SCT, São Paulo, Brazil.

The Vector Harmonic Transform Method for Solving Partial Differential Equations in Spherical Geometry—PAUL N. SWARZTRAUBER, National Center for Atmospheric Research, Boulder, Colorado.

Observing Systems Experiments: Relative Model Response to Various FGGE Datasets in the Tropics—FREDERICK H. CARR, MOHAN K. RAMAMURTHY, DAN J. RUSK, AND GUANG-PING LOU, School of Meteorology, University of Oklahoma, Norman, Oklahoma.

Tornadoes in Chiba Prefecture on 11 December 1990—HIROSHI NIINO, OSAMU SUZUKI, HIROSHI NIRASAWA, TOKUNOSUKE FUJITANI, HISAO OHNO, IZURU TAKAYABU, NOBUYUKI KINOSHITA, Meteorological Research Institute, Tsukuba, Japan; AND YOSHIMITSU OGURA, Ocean Research Institute, University of Tokyo, Nakano, Tokyo, Japan.

Cloud-Shading Retrieval and Assimilation in a Satellite–Model Coupled Mesoscale Analysis System—ALAN E. LIPTON, Atmospheric Sciences Division, Geophysics Directorate, Phillips Laboratory, Hanscom Air Force Base, Massachusetts.

The Use of Partial Cloudiness in a Warm-Rain Parameterization: A Subgrid-Scale Precipitation Scheme—PETER BECHTOLD AND JEAN PIERRE PINTY, Laboratoire d'Aérologie, Université Paul Sabatier, Toulouse, France.

A Case of Downstream Baroclinic Development over Western North America—I. ORLANSKI AND J. SHELDON, Geophysical Fluid Dynamics Laboratory/NOAA, Princeton University, Princeton, New Jersey.

Australian Southerly Busters. Part III: The Physical Mechanism and Synoptic Conditions Contributing to Development—KATHLEEN L. MCINNES, CSIRO, Division of Atmospheric Research, Mordialloc, Victoria, Australia.

Continuous Data Assimilation Experiments with the NMC Eta Model: A GALE IOP 1 Case Study—MOHAN K. RAMAMURTHY AND TAI-YI XU, Department of Atmospheric Sciences, University of Illinois at Urbana–Champaign, Urbana, Illinois.

A Comparative Study of Large-Amplitude Gravity-Wave Events—MOHAN K. RAMAMURTHY, ROBERT M. RAUBER, BRIAN P. COLLINS, AND NARESH K. MALHOTRA, Department of Atmospheric Sciences, University of Illinois at Urbana–Champaign, Urbana, Illinois.

Simulation and Prediction of the Catalina Eddy—KYOZO UEYOSHI AND JOHN O. ROADS, Scripps Institution of Oceanography, University of California, San Diego, La Jolla, California.

A Rain Evaporation and Downdraft Parameterization to Complement a Cumulus Updraft Scheme and Its Evaluation Using GATE Data—Y. C. SUD AND G. K. WALKER, Laboratory for Atmospheres, NASA/Goddard Space Flight Center, Greenbelt, Maryland.

The Influence of Stratiform Precipitation on Shallow Convective Rain: A Case Study—FREDERIC FABRY, ISZTAR ZAWADZKI, AND STEPHEN COHN, J.S. Marshall Radar Observatory and Department of Atmospheric and Oceanic Sciences, McGill University, Montreal, Quebec, Canada.

NOTES AND CORRESPONDENCE

Diabatic Initialization Tests Using the Naval Research Laboratory Limited-Area Numerical Weather Prediction Model—DEWEY E. HARMS, Department of Marine, Earth and Atmospheric Sciences, North Carolina State University, Raleigh, North Carolina; RANGARAO V. MADALA, Naval Research Laboratory, Washington, D.C.; SETHU RAMAN, Department of Marine, Earth and Atmospheric Sciences, North Carolina State University, Raleigh, North Carolina; AND KEITH D. SASHEGYI, Naval Research Laboratory, Washington, D.C.

The Relation between Moist Convective Adjustment Schemes and the Mass-Flux Concept for Cumulus Parameterization—PETER BINDER, Swiss Meteorological Institute, Zurich, Switzerland.

Atlantic Hurricane Season of 1992—MAX MAYFIELD, LIXION AVILA, AND EDWARD N. RAPPAPORT, National Hurricane Center, NWS, NOAA, Coral Gables, Florida.